

Correction: 27 April 2007



www.sciencemag.org/cgi/content/full/1139266/DC1

Supporting Online Material for

Negative Refraction at Visible Frequencies

Henri J. Lezec,* Jennifer A. Dionne, Harry A. Atwater

*To whom correspondence should be addressed. E-mail: lezec@caltech.edu

Published 22 March 2007 on *Science Express*
DOI: 10.1126/science.1139266

This file includes:

SOM Text

Figs. S1 and S2

References

Correction (27 April 2007): The following typos have been corrected:

- 1) Section 1, first paragraph, line 3: $\hat{\mathbf{k}} = \mathbf{k} / k$ replaces $\hat{\mathbf{k}} = |\mathbf{k}| / k$.
- 2) Section 2, line 13: $n_2 = \lambda_0 / P$ replaces $n_2 = 2\lambda_0 / P$.
- 3) Fig. S1, caption: $n_2 = \lambda_0 / P$ replaces $n_2 = 2\lambda_0 / P$.

1. Negative index and negative refraction

Consider an electromagnetic mode propagating with wavevector \mathbf{k} in an isotropic medium. The phase and group velocity of this mode are collinear and given by, respectively, $\mathbf{v}_p = (\omega/k)\hat{\mathbf{k}}$ and $\mathbf{v}_g = (d\omega/dk)\hat{\mathbf{k}}$, where $k = |\mathbf{k}|$, and $\hat{\mathbf{k}} = \mathbf{k}/k$. The phase velocity characterizes the speed and direction of propagation of the phase fronts, whereas the group velocity determines the direction of power flow $\mathbf{S} = \mathbf{E} \times \mathbf{H} = W \mathbf{v}_g$, where \mathbf{S} is the Poynting vector and W is the energy density of the electromagnetic field.

When $d\omega/dk > 0$, \mathbf{v}_p and \mathbf{v}_g are parallel and the standard forward-wave condition $\mathbf{v}_p \cdot \mathbf{v}_g > 0$ is obtained. \mathbf{k} and \mathbf{S} are parallel under such a condition and power propagates in the same direction as the phase-fronts. When $d\omega/dk < 0$, \mathbf{v}_p and \mathbf{v}_g are anti-parallel and the anomalous backward-wave condition $\mathbf{v}_p \cdot \mathbf{v}_g < 0$ is obtained. \mathbf{k} and \mathbf{S} are anti-parallel and power propagates in a direction opposite to that of the phase-fronts.

When a plane wave traveling in medium 1, characterized by phase and group velocities \mathbf{v}_p^1 and \mathbf{v}_g^1 , is incident at an angle φ_1 upon a boundary with medium 2, characterized by phase and group velocities \mathbf{v}_p^2 and \mathbf{v}_g^2 , the resulting refraction angle of the transmitted beam, φ_2 , is dictated by conservation of the parallel component of \mathbf{k} across the boundary as well as conservation of energy (see ref. S1):

$$\frac{\sin(\varphi_2)}{\sin(\varphi_1)} = \frac{\text{sign}(\mathbf{v}_p^1 \cdot \mathbf{v}_g^1) c / |\mathbf{v}_p^1|}{\text{sign}(\mathbf{v}_p^2 \cdot \mathbf{v}_g^2) c / |\mathbf{v}_p^2|} \equiv \frac{n_1}{n_2}. \quad (\text{S1})$$

By analogy with the classical form of the Snell-Descartes law of refraction $\sin(\varphi_2)/\sin(\varphi_1) = n_1/n_2$, an effective refractive index for each medium can be identified based on Eq. S1:

$$n_{1,2} = \text{sign}(\mathbf{v}_p^{1,2} \cdot \mathbf{v}_g^{1,2}) c / |\mathbf{v}_p^{1,2}|. \quad (\text{S2})$$

If $\mathbf{v}_p^i \cdot \mathbf{v}_g^i < 0$, medium i acts as if it had a negative index of refraction. When light exits such a medium into a second medium characterized by a positive index of refraction, it will be refracted, according to Eq. (S1), to the same side of the normal, i.e. to a negative angle.

2. Derivation of mode index of thick Ag/Si₃N₄/Ag waveguide

To derive the actual value of the mode index of the thin Ag/Si₃N₄/Au waveguide, n_1 , the mode index in the surrounding Ag/Si₃N₄/Ag waveguide, n_2 , must be known. To circumvent the difficulty of estimating n_2 theoretically, given the predicted multimodal dispersion properties (Fig. 1A), we measure n_2 directly using an interferometric technique. To this end, Ag/Si₃N₄/Ag waveguides with 500-nm-thick dielectric cores were fabricated with semi-transparent Ag cladding layers of 150nm on each side; no additional Al cladding layer was added. The separation between input and output slit was varied from $d = 1 \mu\text{m}$ to $3 \mu\text{m}$ in 25-nm increments. Each device was illuminated at normal incidence over its entire area and the intensity emitted from the output slit was monitored (Fig. S1 A). Due to interference at the output-slit, between light transmitted along the waveguide and light transmitted directly through the top Ag cladding layer, a periodic modulation in the emitted intensity is obtained as a function of d (Fig. S1 B). At a given wavelength λ_0 , the effective mode index of the waveguide is given by $n_2 = \lambda_0 / P$, where P is the period of the modulation.

3. Effect of thickness and edge angle of Au/Si₃N₄/Ag prism

We characterize in detail the refractive properties of a Ag/Si₃N₄/Au waveguide within its frequency interval of negative refractive index. The result of refraction from a single prism of Ag/Si₃N₄/Au waveguide (W1), of dielectric-core thickness $t_1 = 75 \text{ nm}$, into a thick Ag/Si₃N₄/Ag waveguide (W2), of dielectric core thickness $t_2 = 500 \text{ nm}$, is shown in Fig. S2 A, at two closely-spaced wavelengths of $\lambda_0 = 501 \text{ nm}$ and $\lambda_0 = 488 \text{ nm}$, respectively. Given an incident angle of $\varphi_1 = 7^\circ$ at the W1/W2 interface, substantially different refraction angles $\varphi_2 = -31.2^\circ$ and -27.1° are obtained in each case. Applying Snell's law (Eq. S1) using these angles of refraction and measured values $n_2 = 0.65$ and 0.57 , respectively (Fig. S1 B), we obtain effective refractive indices $n_1 = -2.72$ and -2.09 , respectively. Weak transmission of a positively-refracted spot can also be observed, hinting that 75-nm-thick constrictions can support a strongly attenuated positive-index photonic mode in addition to the negative-index SPP mode. As the waveguide thickness is increased to $t_1 = 150 \text{ nm}$, the positively refracted spot increases in intensity: photonic mode transmission competes with the SPP mode (Fig. S2 B). While the negatively-refracted spot size is slightly reduced with respect to the input slit length, the positively-refracted spot is enlarged. Such variations in spot size likely result from focusing or diffraction effects dependant on both the sign and the magnitude of n_1 .

To confirm the applicability of Snell's law to the bimetallic waveguide structures, we vary the angle of incidence φ_1 by fabricating W1 prisms ($t_1 = 150 \text{ nm}$) with edge angles of $\theta = 5^\circ$ and 7° respectively. Refraction results at $\lambda_0 = 501 \text{ nm}$ are shown in Fig. S2 B. A distinct negatively-refracted spot is obtained in both cases, implying a

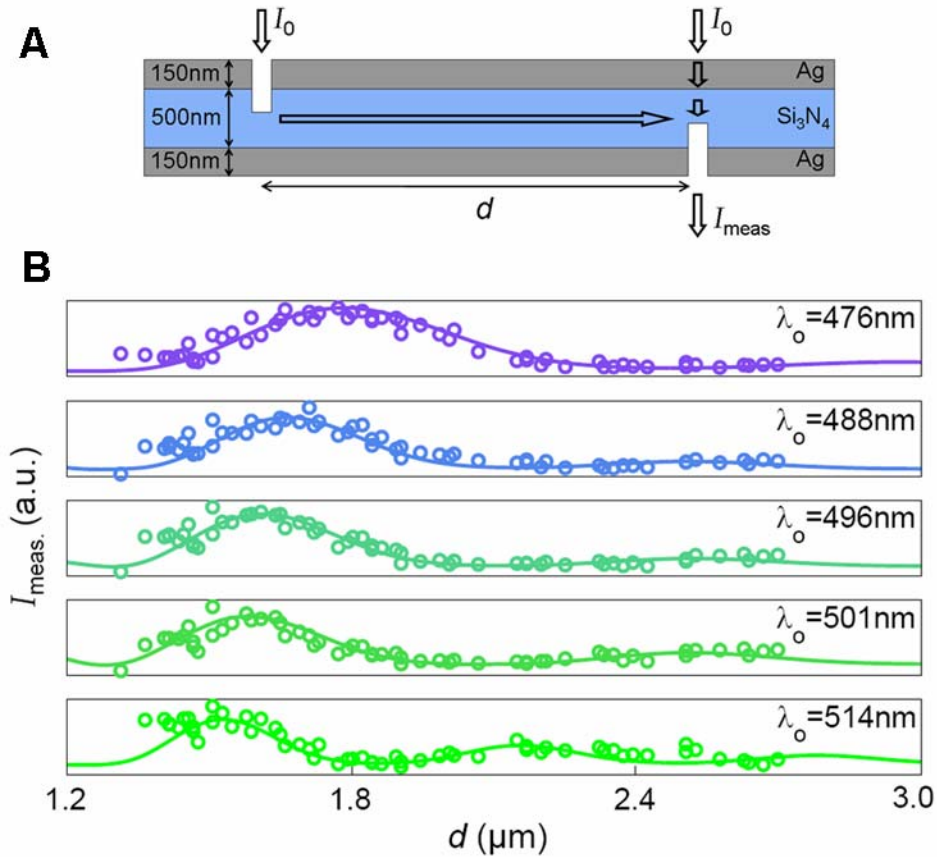


Fig. S1. Experimental determination of refractive index n_2 of thick Ag/Si₃N₄/Ag waveguide. **(A)** Cross-sectional diagram of interferometer used to determine n_2 . The structure is a modified version of the device of Fig 2B, in which the optically opaque metal cladding on both sides of the dielectric core is replaced with a 150-nm-thick layer of Ag. This semi-transparent cladding allows for interference, at the output-slit position, between the transmitted waveguide mode and the partially transmitted incident illumination. Periodic modulation of the light emerging from the output slit as a function of slit-slit distance d yields the effective mode index of the waveguide (S_2). **(B)** Measured output-slit intensity as a function of d for wavelengths within the predicted negative index-region. Distance d is varied from 1 to 3 μm in 25-nm increments. The waveguide index is given by $n_2 = \lambda_0 / P$, where P is the period of modulation. For free-space wavelengths $\lambda_0 = 476, 488, 496, 501, \text{ and } 514 \text{ nm}$, the resulting indices in the Ag/Si₃N₄/Ag waveguide are $n_2 = 0.40, 0.57, 0.50, 0.65, \text{ and } 0.82$, respectively.

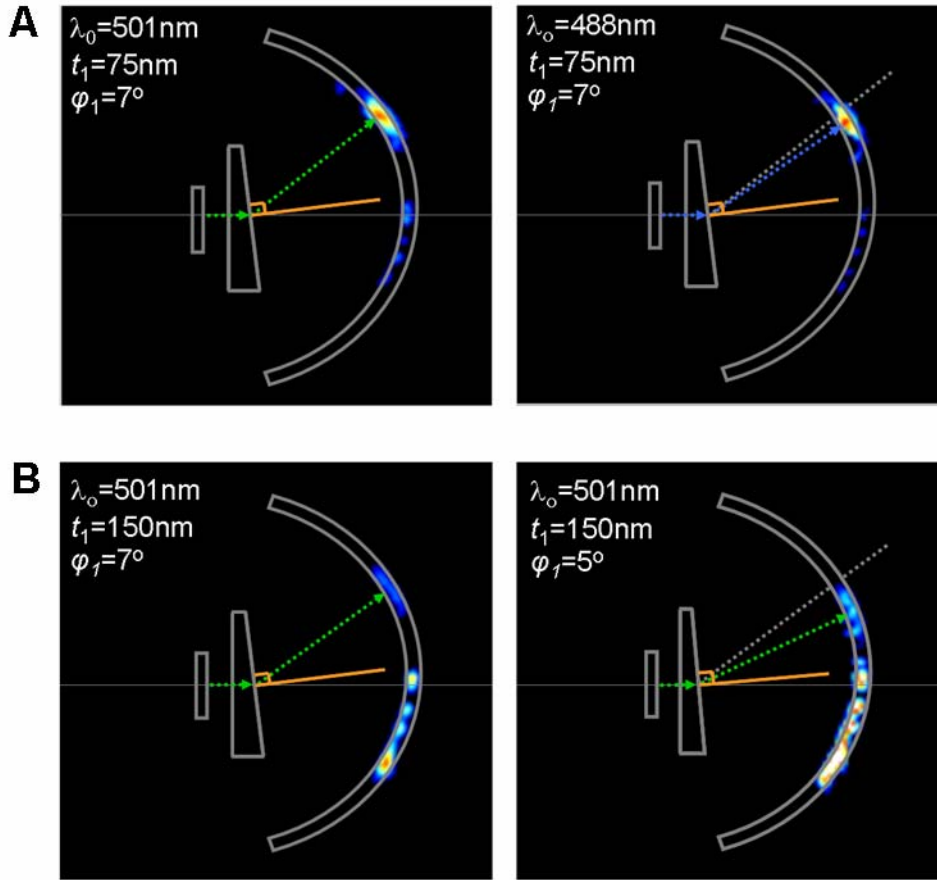


Fig. S2. Detailed exploration of refractive properties of Au/Si₃N₄/Ag waveguide in the negative index region. **(A)** Output-spot position for the single prism geometry of Fig. 2C as a function of wavelength. The core thickness and interface angle of the prism are held constant at $t = 75$ nm and $\theta = \varphi_1 = 7^\circ$, respectively. The angle of refraction φ_2 varies from -31.2° to -27.1° as λ_0 is decreased from 501 to 488 nm. **(B)** Output-spot position for prism angles of $\theta = \varphi_1 = 7^\circ$ and 5° . Here, the core thickness and excitation wavelength are held constant at $t = 150$ nm and $\lambda_0 = 501$ nm, respectively. The angle of the negatively-refracted spot shifts from -28.8° (for $\varphi_1 = 7^\circ$) to -20.0° (for $\varphi_1 = 5^\circ$), corresponding to a constant prism index $n_1 = -2.5$ and confirming the applicability of Snell's Law to such waveguides operating in the negative index region. Note that in both **A** and **B**, bands of positive and negative refraction be observed, corresponding to transmission of a positive-index photonic mode and a negative-index plasmonic mode, respectively.

refraction angle of $\varphi_2 = -20.0^\circ$ when $\varphi_1 = 5^\circ$ and of $\varphi_2 = -28.8^\circ$ when $\varphi_1 = 7^\circ$. The corresponding ratio $\sin(\varphi_2)/\sin(\varphi_1) = n_1/n_2$ is -3.82 and -3.88 , respectively. The constancy of this ratio as a function of edge angle implies that Snell's law indeed applies to the present structures operating in the negative index region.

References

- S1. V. G. Veselago, *Sov. Phys. Usp.* **10**, 509 (1968).
- S2. J. A. Dionne, H. J. Lezec, H. A. Atwater, *Nano Lett.* **6**, 1928 (2006).